Brain Stimulation 14 (2021) 379–388

Contents lists available at ScienceDirect

Brain Stimulation

journal homepage: http://www.journals.elsevier.com/brain-stimulation

Asymmetric transcallosal conduction delay leads to finer bimanual coordination

Marta Bortoletto [a, *], Laura Bonzano [b], Agnese Zazio [a], Clarissa Ferrari [c], Ludovico Pedullà [d], Roberto Gasparotti [e], Carlo Miniussi [f], Marco Bove [d, g, **]

[a] Neurophysiology Lab, IRCCS Istituto Centro San Giovanni di Dio Fatebenefratelli, Brescia, Italy
[b] Department of Neuroscience, Rehabilitation, Ophthalmology, Genetics, Maternal and Child Health, University of Genoa, Genoa, Italy
[c] Statistics Unit, IRCCS Istituto Centro San Giovanni di Dio Fatebenefratelli, Brescia, Italy
[d] Department of Experimental Medicine, Section of Human Physiology, University of Genoa, Genoa, Italy
[e] Department of Medical and Surgical Specialties, Radiological Sciences, And Public Health, Section of Neuroradiology, University of Brescia, Brescia, Italy
[f] Center for Mind/Brain Sciences CIMeC, University of Trento, Rovereto, Italy
[g] Ospedale Policlinico San Martino-IRCCS, Genoa, Italy

ARTICLE INFO

Article history:
Received 5 August 2020
Received in revised form
8 January 2021
Accepted 4 February 2021
Available online 10 February 2021

Keywords:
Information transfer
Effective connectivity
Interhemispheric inhibition
TMS-EEG
DTI

ABSTRACT

It has been theorized that hemispheric dominance and more segregated information processing have evolved to overcome long conduction delays through the corpus callosum (transcallosal conduction delay - TCD) but that this may still impact behavioral performance, mostly in tasks requiring high timing accuracy. Nevertheless, a thorough understanding of the temporal features of interhemispheric communication is lacking.

Here, we aimed to assess the relationship between TCD and behavioral performance with a non-invasive directional cortical measure of TCD obtained from transcranial magnetic stimulation (TMS)-evoked potentials (TEPs) in the motor system.

Twenty-one healthy right-handed subjects were tested. TEPs were recorded during an ipsilateral silent period (iSP) paradigm and integrated with diffusion tensor imaging (DTI) and an in-phase bimanual thumb-opposition task. Linear mixed models were applied to test relationships between measures.

We found TEP indexes of transcallosal communication at ~15 ms both after primary motor cortex stimulation (M1-P15) and after dorsal premotor cortex stimulation (dPMC-P15). Both M1-and dPMC-P15 were predicted by mean diffusivity in the callosal body. Moreover, M1-P15 was positively related to iSP. Importantly, M1-P15 latency was linked to bimanual coordination with direction-dependent effects, so that asymmetric TCD was the best predictor of bimanual coordination.

Our findings support the idea that transcallosal timing in signal transmission is essential for interhemispheric communication and can impact the final behavioral outcome. However, they challenge the view that a short conduction delay is always beneficial. Rather, they suggest that the effect of the conduction delay may depend on the direction of information flow.

Introduction

Conduction delay over long-range connections is a crucial feature of neural communication that impacts the efficacy of signal transmission between distant areas and thus influences the anatomo-functional brain architecture. Specifically, long transcallosal conduction delay (TCD) has been theorized to be the basis of hemispheric dominance: long TCD prevents the exchange of information between homologous cortical areas and favors the compartmentalization of signal processing [1–3]. Such delays impact each transcallosal information transfer regardless of the information conveyed, i.e., both when the processes of the two hemispheres must be integrated and when the two hemispheres exert mutual functional inhibition, possibly directed toward suppression of competing activation, as shown in the motor system [4].

* Corresponding author. Neurophysiology Lab, IRCCS Istituto Centro San Giovanni di Dio Fatebenefratelli, Via Pilastroni 4, 25125, Brescia, Italy.
** Corresponding author. Department of Experimental Medicine, Section of Human Physiology, University of Genoa, Viale Benedetto XV 3, 16132, Genoa, Italy.
E-mail addresses: marta.bortoletto@cognitiveneuroscience.it (M. Bortoletto), marco.bove@unige.it (M. Bove).

https://doi.org/10.1016/j.brs.2021.02.002

The impact of TCD on interhemispheric signal transmission may eventually have consequences on behavioral performance, becoming most apparent when tasks have strict timing constraints [1].

Despite the acknowledged importance of TCD in brain functioning and initial indications that TCD affects cognitive functions [5,6], empirical support has been limited to date due to the lack of a direct noninvasive measure of TCD. Pioneering studies have exploited lateralized effects on reaction times and event-related potentials, but these effects may be affected by several stages along the processing stream [7–9]. In relation to the motor system, estimates of TCD have been obtained with peripheral measures of transcallosal inhibition, such as the ipsilateral silent period (iSP) [10–14], but they are affected by the corticospinal tract. Finally, double-coil TMS studies can provide measures of TCD, but they require a high number of pulses to reach high precision at the single subject level [4,15]. Overall, the estimates of TCD are not fully consistent across different approaches: the onset of inhibition between primary motor cortices (M1s) has been estimated around 7–8 ms for double coil studies [4] and around 15–20 ms for iSP paradigms [10–12]. Consequently, it is not well understood how conduction delay in transcallosal connections affects lateralized processing and behavioral outcomes.

Coregistration of transcranial magnetic stimulation (TMS) and electroencephalography (EEG) has the potential to provide temporally precise cortical measures of effective connectivity through TMS-evoked potentials (TEPs): After the direct activation of a target region at the time of TMS, a secondary neural response is generated in distant connected regions, e.g., a homologous area connected via the corpus callosum (CC), and this response is recorded through EEG [16]. The amplitude and latency of the secondary response can be measured from the TEPs and reflect the strength and conduction delay of the connection, respectively. Importantly, TEPs can provide directional information in the communication between the two hemispheres, allowing us to explore the relative contribution of the dominant and the nondominant hemispheres.

In this work, we hypothesized that an early contralateral component of TEPs could represent the response of the area contralateral to the stimulated one [17–19] after signal transmission through callosal fibers, with its latency providing an index of TCD. We tested our hypothesis by relating the earliest TEP component, occurring at approximately 15 ms (M1-P15), after M1 stimulation with the iSP and DTI measures of the CC. First, if M1-P15 amplitude reflects inhibition of the contralateral M1, it should be positively associated with the magnitude of iSP. Second and most importantly, if M1-P15 latency reflects TCD, it should be related to the diffusivity of water molecules in the fibers of the callosal body, i.e., the CC section connecting homologous motor cortices. As a control analysis, we tested the generalization of this approach to another area of the motor system, i.e., whether the earliest TEP component is generated after stimulation of the dorsal premotor cortex (dPMC) can provide a measure of TCD. Given that the callosal fibers connecting the dPMC are just anterior or even intermingled with callosal fibers connecting the M1s [20], we expected a relationship with the body of the CC.

As our results supported that M1-P15 and dPMC-P15 latencies provide an index of TCD, we tested the hypothesis that TCD and behavioral performance are associated when interhemispheric activity has to be tuned with high timing accuracy. TEPs allowed us to test our hypothesis separately for each direction of information transfer, i.e., from the left-to-right hemisphere and from the right-to-left hemisphere. According to the interhemispheric independence hypothesis [1], a higher TCD should increase the time lag between hands, reducing bimanual coordination, while possible effects of the direction of interhemispheric transfer are not explicitly taken into account.

As a behavioral task, we adopted a bimanual in-phase coordination task based on sequences of finger opposition movements that are influenced by callosal integrity in multiple sclerosis [21] and in callosotomy and agenesis of CC [22,23]. Specifically, bimanual in-phase coordination has been shown to depend on M1 activity and interhemispheric connectivity [24,25]. In contrast, studies on dPMC reported no evidence for a key role for hand coordination in this kind of movement 25,26. Therefore, we expected that M1-P15 would predict bimanual performance.

Materials and methods

Participants

Twenty-one right-handed healthy participants with no history of neurological disorders or contraindications to magnetic resonance imaging (MRI) and TMS gave written informed consent and participated in the study. One participant was excluded from analyses due to technical problems during data acquisition. The final sample characteristics were as follows: mean age 34 years (range 26–47 years); 9 females; Edinburgh Handedness Inventory [27], mean ± SE: 82.1 ± 3.6. The study included two sessions within two weeks: MRI examination including DTI (Session 1; Fig. 1a) and behavioral tasks and TMS-EEG for TEPs and iSP recording (Session 2; Fig. 1b–d). The study was performed in accordance with the ethical standards of the Declaration of Helsinki and was approved by the Ethical Committee of the IRCCS Istituto Centro San Giovanni di Dio Fatebenefratelli (Brescia) and by the Ethical Committee of the Hospital of Brescia.

Session 1

MRI was performed on a 3 T MR system (Skyra, Siemens, Erlangen, Germany), including axial T2-weighted fluid-attenuated inversion recovery (FLAIR; repetition time (TR) 9000 ms, echo time (TE) 76 ms, inversion time (TI) 2500 ms, slice thickness 3 mm, distance factor 10%, 1 average, field of view (FOV) 220 mm, voxel size 0.6 × 0.6 × 3.00 mm), DTI with spin-echo echo-planar axial sequences (multiband, TR 4100 ms, TE 75.0 ms, 1.8 mm isotropic resolution, b 1000 s/mm^2, 64 encoding directions, 5 b0 images, fat suppression), and high-resolution T1-weighted 3D anatomical sequences (sagittal volume, TR 2400 ms, TE 2 ms, 0.9 mm isotropic resolution).

Session 2

Participants were comfortably seated in a dimly lit room in front of a computer screen, resting their forearms on a table, and wearing an EEG cap and two engineered gloves (GAS, ETT, s.p.a., Genoa, Italy) [28–30]. The gloves detected the onset and the offset of single touches in each hand. The interhand interval was then calculated as the timing intervals between the corresponding touch onsets of the two hands.

First, participants performed two metronome-paced in-phase bimanual tasks at 2 Hz: simple mirror-symmetrical thumb-to-index-finger opposition and sequential mirror-symmetrical thumb-to-finger opposition tasks (Fig. 1b) [21]. Each condition was performed twice in separate runs lasting 45 s and separated by a few minutes of rest to avoid fatigue.

Then, the maximum muscle contraction of each abductor pollicis brevis (APB) was measured for 30 s. The maximum value in this recording was subsequently analyzed to calculate the relative contraction levels during TMS-EEG.

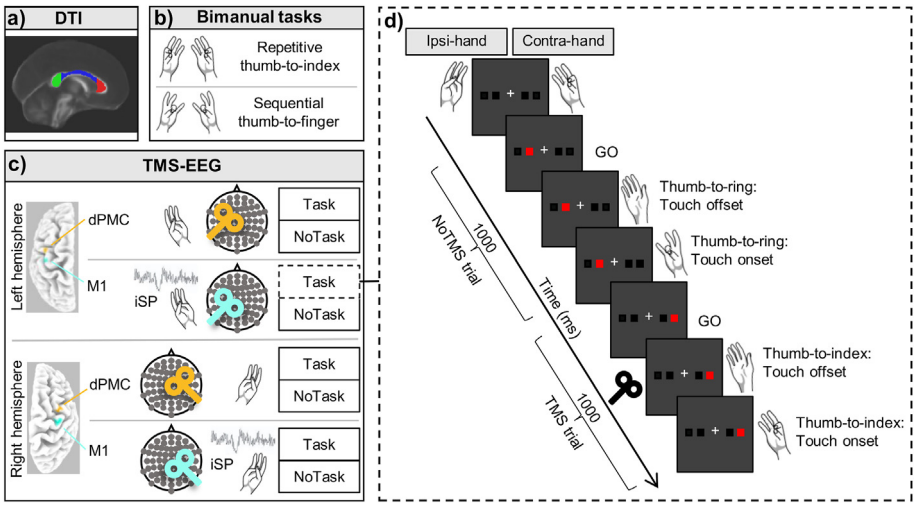

Fig. 1. Study methods. Experimental procedure consisting of DTI acquisition, in-phase bimanual coordination tasks and TMS-EEG and iSP recording. a) From DTI, mean fractional anisotropy and mean diffusivity were calculated in three regions of the corpus callosum: the genu (red), the body (blue), and the splenium (green). b) Bimanual tasks included simple finger tapping (thumb-to-index-finger opposition) and 4-item sequential finger tapping (thumb-to- index, middle, ring and little fingers). c) During TMS-EEG, the left M1, left dPMC, right M1 and right dPMC were stimulated in separate blocks in an iSP paradigm. The averaged hotspots are shown on the left side of the panel. The iSP paradigm involved Task and NoTask conditions in counterbalanced order. During both conditions, the thumb and the little finger of the ipsilateral hand were opposed, maintaining a slight contraction of the APB. In the Task condition, participants performed the unimanual finger opposition movement sequence described in d). In the NoTask condition, they saw the same stimuli as in the Task condition, but they were not required to perform a tapping task with the contralateral hand. d) Two example trials of the Task condition, comprising one trial without and one trial with TMS over the left M1. Participants were presented with four white squares on the distal phalanges of the index, middle, ring and little fingers. The white squares turned red one at a time in random order, and participants were instructed to respond as quickly and accurately as possible by opposing the thumb to the corresponding finger. The block started with participants in a resting position, touching the tip of the index finger to the tip of the thumb. Upon the presentation of the stimuli, participants lifted their fingers (touch offset) and tapped their thumb to the finger indicated by the stimulus (touch onset). Stimuli lasted 1000 ms and were presented at a frequency of 1 Hz. The number of stimuli per block was 120. (For interpretation of the references to colour in this figure legend, the reader is referred to the Web version of this article.)

Finally, participants underwent TMS-EEG recording (Fig. 1c). Single biphasic TMS pulses were delivered with a C-B60 coil (MagPro X100 including MagOption, MagVenture) over the left and right hemispheres, targeting M1 or dPMC in counterbalanced order. The coil was positioned tangentially to the scalp with the handle pointing backward and rotated away from the midline by approximately 45°, inducing an anterior-to-posterior and posterior-to-interior (AP-PA) current direction in the cortex. The M1 hotspot was functionally localized as the position that induced reliable motor evoked potentials (MEPs) in the APB. To stimulate dPMC, the target was moved forward 15 mm from the individual M1 coordinates, in accordance with coordinates of peak activation of M1 and dPMC during motor tasks [31]. Target positions were visually monitored on individual T1 images displayed in the neuronavigation system. The coordinates of the hot spots are reported in Table S1.

TMS-EEG was recorded while participants underwent an iSP paradigm including two conditions (Task and NoTask) to increase the range of motor inhibition [32]. The hand contralateral to the stimulation performed a unimanual finger tapping task in the Task condition (Fig. 1d) or was relaxed in the NoTask condition. In the hand ipsilateral to the stimulation, the thumb and the little finger were opposed and contracted in both conditions. The instruction was to perform a light contraction to allow iSP recording while avoiding fatigue (details of task performance and contraction level can be found in Tables S2–S3). The experimenter visually monitored EMG activity during the task and asked participants to increase their contraction level when it looked too low. Before the recording, participants performed a training block with each hand to familiarize with the task. TMS was randomly delivered in half of the trials, i.e., in 60 pulses per block, based on individual task performance which was sent from the engineered gloves to the computer that controlled stimuli presentation and TMS delivery: in the Task condition, TMS was delivered at the time of touch offset in the hand performing the task, i.e., their reaction time; To stimulate in a similar way in the NoTask condition, in which the contralateral hand was resting and no touch offset could be measured, TMS was delivered in a window of 200 ms around the average time of touch offset, as measured in the training block. TMS intensity (mean ± SE: 58.1% of MSO ± 1.6%) was set at 110% of the individual average resting motor threshold [33], and recharge delay was 500 ms. This TMS intensity was chosen for being high enough to evoke MEPs in the majority of trials in both Task and NoTask conditions but not too high to create discomfort in the Task condition when participants were moving their contralateral hand. Stimulation was assisted by a neuronavigation system (SofTaxic, EMS, Italy), coregistering the T1 anatomical MRI to head position.

A TMS-compatible system (BrainAmp, Brain Products GmbH, Munich, Germany) was employed to record 67-channel EEG (reference to the nose, ground at FPz), vertical and horizontal electrooculogram (EOG) and electromyography (EMG) from the APBs of both hands using two pairs of surface electrodes with a belly tendon montage. Amplifiers were set with a 5 kHz sampling rate and online 0.1–1000 Hz bandpass filter. Impedance was below 5 kΩ. These settings allowed us to record a TMS artifact as short as 5 ms [34].

Diffusion tensor imaging (DTI)

DTI data were processed using FMRIB's Diffusion Toolbox [35]. After correction for eddy current and motion artifacts, a diffusion tensor model was fitted at each voxel, and the three eigenvalues were calculated [36]. Parametric maps were obtained for fractional anisotropy, a measure indicating the overall directionality of water diffusion within brain tissue, and mean diffusivity (MD) which describes the rotationally invariant magnitude of water diffusion independent of anisotropy [37,38]. These maps were nonlinearly transformed and aligned to 1 × 1 × 1 mm standard space using

tract-based spatial statistics routines [39]. To assess the microstructural properties of the CC, the mean value of each DTI-derived parameter was calculated for each scan in the voxels included in the callosal fibers within three regions of interest (genu, body, and splenium) from the JHU ICBM 81 white matter label atlas [40].

Although more sophisticated techniques for diffusion imaging are available, we chose a validated and reproducible approach based on the subdivision of the CC in three regions of interest defined within a validated atlas of white matter tracts, which allows comparing the different DTI-derived parameters in the same number of voxels in an automated manner in all subjects, as in Ref. [37].

Bimanual coordination

Bimanual coordination performance was measured as the absolute interhand interval for each tap, i.e., the unsigned time difference between the onset of finger tap with the left hand and the onset of the corresponding finger tap with the right hand (interhand interval values > 2 SD were excluded). Therefore, the longer the interhand interval, the worse the bimanual coordination [21]. The data were log-transformed to obtain a normal distribution. Data from one participant were missing due to technical problems with the gloves.

TMS-evoked potentials (TEPs)

TMS-EEG data analysis was performed in MATLAB (The MathWorks, Natick, MA, USA) with custom scripts using EEGLAB [41] and FieldTrip functions [42] and two analysis methods, namely, the source-estimate-utilizing noise-discarding (SOUND) algorithm [43] and the signal-space projection and source-informed reconstruction (SSP-SIR) algorithm [44]. These algorithms are suitable for separating TMS-related cortical activity from TMS-related artifacts because they do not rely on the assumption that the signal and the artifacts are independent. Moreover, there is evidence that SSP-SIR performs well for removing sensory-related signals while preserving data [45]. Continuous EEG was interpolated around the TMS pulse (from −1 ms to 6 ms), high-pass filtered (0.1 Hz), epoched (from −200 ms to 500 ms) and downsampled to 2048 Hz. Measurement noise was discarded with SOUND (spherical 3-layer model, regularization parameter: $\lambda = 0.01$). Then, the following steps were performed: visual inspection, artifact rejection, and independent component analysis (ICA; infomax algorithm) for ocular artifact correction. Subsequently, TMS-evoked muscular artifacts in the first 50 ms were removed using SSP-SIR (0–3 muscle-artifact components in each dataset). Then, epochs were low-pass filtered at 70 Hz and rereferenced to the average of TP9-TP10. Finally, after a second visual inspection and artifact rejection, TMS-EEG data were baseline corrected from −100 ms to −2 ms before the TMS pulse and averaged. At the end of the preprocessing pipeline, the average number of trials in each condition was between 57 and 59. P15 was identified as the first TEP component over the hemisphere contralateral to stimulation in the grand average of all conditions for M1 stimulation and dPMC stimulation. The peak location corresponded to contralateral frontocentral channels (F2-FC2 for left M1-TMS, F1-FC1 for right M1-TMS; F2-FC2-F4-FC4 for left dPMC-TMS, and F1-FC1-F3-FC3 for right dPMC-TMS). After pooling these electrodes, we measured amplitude and latency for each individual as the first positive peak between 5 and 30 ms.

Ipsilateral silent period (iSP)

iSP parameters were assessed in the trace obtained by averaging the 60 rectified EMG traces recorded during M1-TMS [11]. No iSP was measured for dPMC-TMS because, to our knowledge, iSP after dPMC stimulation has not been investigated before. The following iSP parameters were considered: the iSP onset, defined as the point after cortical stimulation at which EMG activity became constantly (for a minimum duration 10 ms) below the mean amplitude of EMG activity preceding the cortical stimulus; the iSP duration, calculated by subtracting the onset time from the ending time (i.e., the first point after iSP onset at which the level of EMG activity returned to the mean EMG signal); and the normalized iSP area, calculated using the following formula: [(area of the rectangle defined as the mean EMG × iSP duration)−(area underneath the iSP)] divided by the EMG signal preceding the cortical stimulus. The normalized iSP area is a stable measure and is independent of the contraction level in the ipsilateral muscles [46].

Statistical analysis

To account for the hierarchical structure of the design, involving repeated measures within subjects, relationships between variables were tested by linear mixed models (LMMs) with random slopes and intercepts [47]. Based on the experimental design and on the specific investigation hypothesis, we took into account both i) the variability of each subject with his/her specific starting point and ii) the variability of the repeated measures within each condition so that all LMMs included random slopes and intercepts. The inclusion of repeated measures in LMMs contributes to and increases statistical power without inflating the number of observations. A summary is reported in Tables S4–S5. The Akaike information criterion (AIC) was used to find the best model in terms of goodness of fit. In case of more than one model with the same dependent variable were significant, the AIC was used to choose the best predictor of the dependent variable in the analysis.

To test the relationship between M1-P15 amplitude (repeated independent variable) and iSP normalized area (repeated dependent variable), an LMM was run with condition (4 levels: Task, NoTask, LeftTMS, RightTMS) and subject as fixed and random effects, respectively, with each condition repeated within subjects. The same model was employed to evaluate the relationship between M1-P15 latency and iSP onset.

To study the predictive value of the microstructural integrity of the CC body (i.e., DTI measures as independent variables) on M1-P15 latency (dependent variable), two separate LMMs were applied for fractional anisotropy and mean diffusivity of the CC body. In addition, the mean diffusivity for other CC regions was evaluated by carrying out two other LMMs with M1-P15 latency as the dependent variable and CC genu and CC splenium as predictors.

Finally, we tested the relationship between M1-P15 latency (as predictor) and bimanual coordination performance (i.e., interhand interval, as dependent variable) in a sequential thumb-to-finger opposition movement task. Separate LMMs were performed considering the three measures of M1-P15 latency (i.e., mean value of Task and NoTask condition in the left TMS and right TMS and the ratio between the two) as predictors, each tap of the bimanual task as a fixed effect and subject as a random effect (with taps repeated within subjects).

The same LMMs were applied to test the relationship between dPMC-P15 latency and DTI measures and the relationship between dPMC-P15 latency and interhand interval. No relationship was tested between dPMC-P15 and iSP.

Statistical significance was set at $p < 0.05$. All analyses were performed in R software [48], and LMMs were estimated by the lme4 package.

Finally, to control that TMS applied over M1 and over dPMC evoked different cortical responses, TEPs were compared by means of cluster-based permutation tests for dependent samples in MATLAB (The MathWorks, Natick, MA, USA) with FieldTrip functions [39] (Fig. S1).

Results

TMS over the targeted M1 induced a complex TEP response (Fig. 2a), including an early component peaking at approximately 15 ms over contralateral frontocentral sites, i.e., the above-mentioned M1-P15. P15 latency is in line with estimates of TCD from anatomical studies [2,49] and double-coil TMS studies [4]. The positive polarity is in line with the relationship between positivity and inhibition that has been shown in motor areas. Importantly, M1-P15 was highly consistent and could be detected in every condition (Fig. 2b and c), as was iSP (Table S6).

Interestingly, the stimulation of dPMC generated another contralateral positive component at approximately 15 ms (dPMC-P15) (Fig. 3a–c; Table S7).

M1-P15 amplitude predicts the magnitude of iSP

First, M1-P15 was linked to contralateral motor inhibition: LMM showed that M1-P15 amplitude predicts the normalized iSP area ($t = 4.09$, $p<0.001$), i.e., the larger the M1-P15, the stronger the inhibition in the ipsilateral APB (Fig. 2d). Our results do not provide evidence for a causal relationship between M1-P15 amplitude and the magnitude of iSP; Rather, they support that both measures reflect the amount of inhibition induced by the activation of the contralateral M1, as has already been demonstrated for the iSP [11,13,14]. The relationship between M1-P15 latency and iSP onset did not reach the a priori level of significance ($t = 1.8$, $p = 0.08$; Fig. S2).

Finally, we ran the same LMM with dPMC-P15 amplitude as an independent variable, and we found no significant relationship ($t = 1.5$, $p = 0.14$, Fig. S3), suggesting that the relationship between P15 amplitude and iSP area is specific for M1 stimulation.

M1-P15 latency is predicted by mean diffusivity of the CC body

As evidence that M1-P15 reflects the timing of transcallosal connectivity, we assessed whether CC microstructural integrity predicts M1-P15 latency. A summary of all results can be found in Table S4. We found that M1-P15 latency was predicted by the mean diffusivity of the CC body ($t = -3.12$, $p = 0.005$; Fig. 2e): the higher the mean diffusivity, the shorter the M1-P15 latency, i.e., shorter TCD. No significant relationship was found for splenium and genu (Figs. S4a–b), supporting that the relationship was specific for the callosal body and not for the other regions. Although our study does not provide evidence of a causal relationship between diffusivity and M1-P15 latency, it is reasonable to believe that diffusivity along the CC is responsible for M1-P15 latency (and not vice versa).

dPMC-P15 latency is predicted by mean diffusivity of the CC body

As additional evidence that the stimulation of a motor area can induce transcallosal spread of signals to the other hemisphere, we tested the relationship between dPMC-P15 latency and DTI. A summary of results can be found in Table S5. Interestingly, dPMC-P15 was also specifically associated with the mean diffusivity ($t = 2.67$, $p = 0.02$; Fig. 3d) of the CC body and not with DTI measures of other CC regions.

Directional M1-P15 latency predicts bimanual coordination

Our next goal was to test how TCD is related to behavior. Based on the interhemispheric independence hypothesis [1] and previous studies [21], we expected that TCD between homologous motor areas could affect the temporal precision of motor performance when bilateral movements must be coordinated. Moreover, we explored whether such a relationship was present for each direction of interhemispheric transfer, i.e., for left-to-right and for right-to-left information transfer. We found that M1-P15 latency from the left-to-right hemisphere positively predicted the interhand interval ($t = 2.88$, $p = 0.007$; Fig. 4a), such that a shorter TCD resulted in a shorter interhand interval, i.e., better bimanual coordination. In the opposite direction, the relationship between the right-to-left M1-P15 latency and the interhand interval, showed a negative trend that did not reach significance level fixed at $p < 0.05$ ($t = -1.71$, $p = 0.09$; Fig. 4b). Finally, the ratio of the M1-P15 latency from the dominant (left) M1 to the M1-P15 latency from the nondominant (right) M1 ($t = 5.36$, <0.001; Fig. 4c) predicted bimanual coordination as indicated by the AIC method [50,51].

As a control condition, we tested the relationship between M1-P15 latency and interhand interval during bimanual simple thumb-to-index-finger opposition movements, in which the CC seems to be less involved [52]. No statistical significance was found (left TMS: $t = 0.31$, $p = 0.76$; right TMS: $t = -1.37$, $p = 0.18$; left/right TMS: $t = 1.37$, $p = 0.18$; Fig. S5).

Finally, we tested the relationship between dPMC-P15 and interhand interval and found no significant results.

These data show that sequential bimanual coordination is associated with TCD between homologous motor areas. Importantly, asymmetric TCD, when signal transmission from M1 in the dominant hemisphere to the nondominant hemisphere is faster than transmission in the opposite direction, is the best predictor of bimanual coordination performance.

Discussion

Our results introduce evidence that TEP components occurring approximately 15 ms after motor area stimulation (M1-P15 and dPMC-P15) reflect transcallosal signal transmission to contralateral areas. Indeed, M1-P15 latency and dPMC-P15 latency are inversely related to the magnitude of water diffusion in the fibers of the callosal body. Moreover, M1-P15 amplitude is positively related to inhibition of the contralateral M1 as measured by iSP. With this new measure of TCD, we are able to reveal that TCD significantly predicts bimanual coordination and that this relationship depends on the stimulated hemisphere. Specifically, asymmetry in TCD between M1s is associated with better bimanual coordination: shorter left-to-right TCD and longer right-to-left TCD after M1-TMS resulted in better temporal performance in bimanual finger opposition movements.

The relationship between TEP latency and the mean diffusivity of the callosal body is a crucial finding to support that TEPs reflect the TCD (Fig. 1e). Importantly, regardless of the specific underlying anatomical characteristics, higher water diffusivity can reflect better signal propagation. A TEP-based estimate of TCD may be very close to the actual TCD of the fiber tract, although it may be slightly overestimated due to the time required for TMS to activate pyramidal neurons in the target region, which takes less than 1 ms [53], and the time required for activation of local circuits in the connected area, which has been estimated to be approximately 1–2 ms. Moreover, it is noteworthy that TCD was measured as the

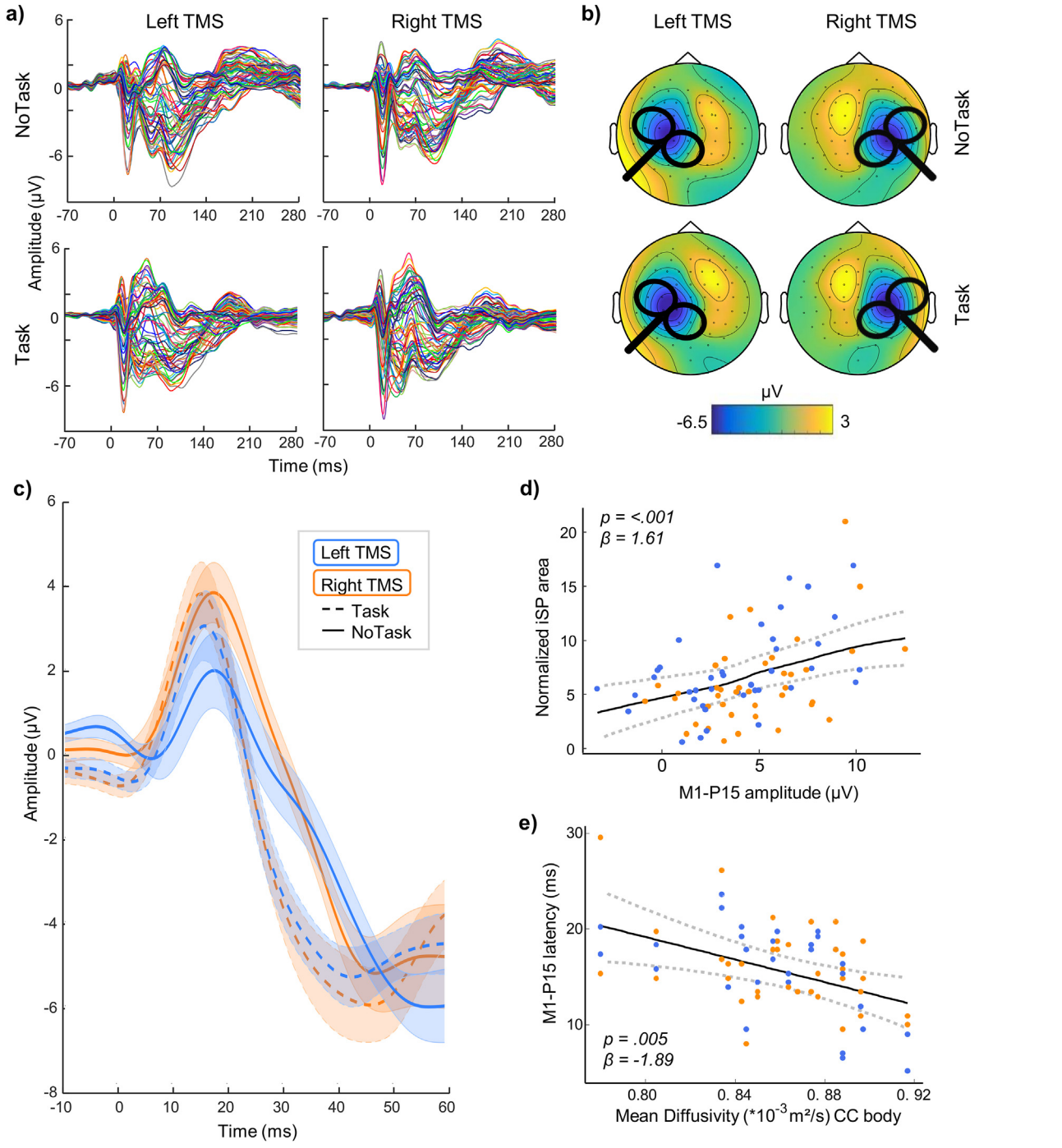

Fig. 2. M1-P15 as a measure of transcallosal effective connectivity. a) Grand average of TEPs in the four experimental conditions. b) Topographical maps of M1-P15 showing a consistent pattern of positive activation in frontal electrodes contralateral to TMS in the four experimental conditions. c) Grand average of M1-P15 in the four experimental conditions (SE represented by shaded error bars). M1-P15 was identified in each participant and each condition as the first positive peak within a 5–30 ms interval in pooled data from two frontal electrodes contralateral to the TMS site (F1 and FC1 for right TMS, F2 and FC2 for left TMS). d) Relationship between M1-P15 amplitude and normalized iSP area: higher M1-P15 is associated with greater iSP. e) Relationship between mean diffusivity in the body of the CC and M1-P15 latency: higher mean diffusivity predicts shorter M1-P15 latency. In d) and e), blue dots indicate left TMS, and orange dots indicate right TMS. Data from the Task and NoTask conditions were pooled together. Fitted curves were drawn by applying a smoothed spline to predicted values—obtained by a bootstrap procedure with n = 500 simulations—in the LMMs. Dashed lines represent the 95% confidence interval. (For interpretation of the references to colour in this figure legend, the reader is referred to the Web version of this article.)

peak of P15. Therefore, it is unlikely that we measured the beginning of the inhibition, i.e. the delay of the fastest callosal fibers. Rather, P15 latency may be closer to the delay at which the inhibition arrives from most callosal fibers. This may explain the overestimation compared to double-coil TMS studies [4,54] and the agreement with anatomical studies [2,49] where TCD is estimated based on the population of axons and with other TMS protocols, like paired associative stimulation [55].

Interestingly, in previous studies on bimanual coordination, in which participants were instructed to synchronize their upper limb

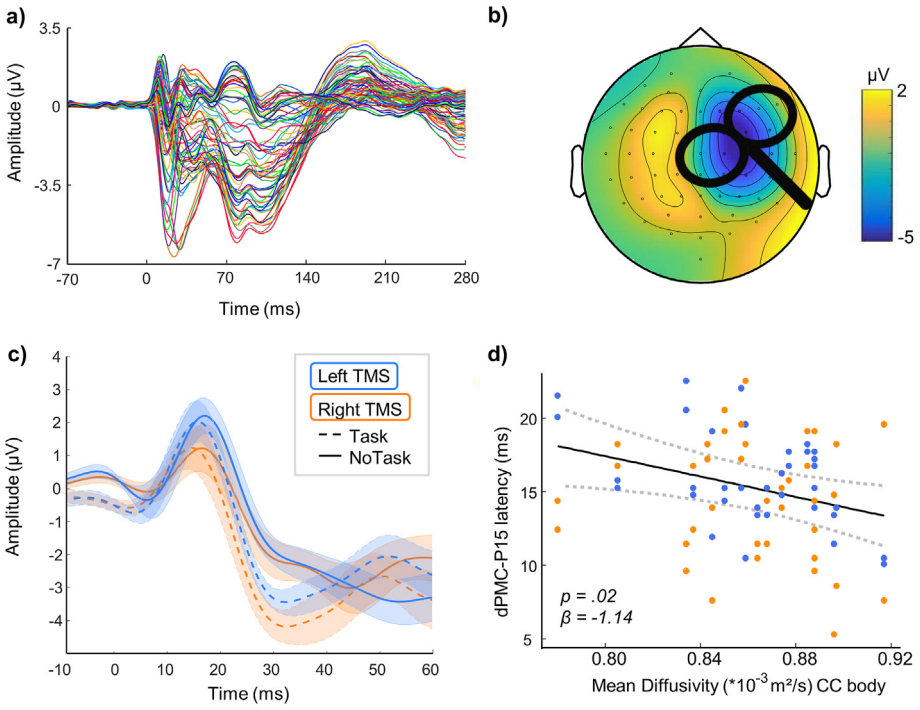

Fig. 3. dPMC-P15 as a measure of transcallosal effective connectivity. a) Grand average of TEPs after dPMC-TMS. b) Topographical maps of dPMC-P15 showing positive activation in frontal electrodes contralateral to TMS. For display purposes, in a) and b), the four conditions (left and right M1-TMS and dPMC-TMS) are collapsed together (data after left dPMC-TMS have been flipped to right side for visualization purposes). c) Grand average of dPMC-P15 in the four experimental conditions (SE represented by shaded error bars). dPMC-P15 was identified in each participant, and each condition was the first positive peak within a 5–30 ms interval in pooled data from four frontal electrodes contralateral to the TMS site (F1, F3, FC1, FC3 for right TMS; F2, F4, FC2, FC4 for left TMS). d) Relationship between mean diffusivity in the CC body and dPMC-P15 latency: higher diffusivity predicts shorter dPMC-P15 latency (blue dots indicate left TMS, and orange dots indicate right TMS). Data from the Task and NoTask conditions were pooled together. A fitted curve was drawn by applying a smoothed spline to predicted values—obtained by a bootstrap procedure with n = 500 simulations—in the LMMs. Dashed lines represent the 95% confidence interval. (For interpretation of the references to colour in this figure legend, the reader is referred to the Web version of this article.)

movements, it was found that the dominant limb led the non-dominant limb during the production of bimanual circle or line drawing with a time delay of about 15–20 ms [56–58].

Crucially, our findings support that temporal features in the communication between hemispheres shape the final behavioral outcome (Fig. 3). However, how this occurs may be different from what is expected from current theories. The timing of information transfer is at the heart of the interhemispheric independence hypothesis [1], which states that a long TCD limits the exchange of information between hemispheres in both directions and that such delay is burdensome in tasks requiring millisecond timing accuracy. Nevertheless, it is overlooked that TCD may be different in each direction of information transfer, and it is implied that a long TCD is always detrimental to behavioral outcomes. Evidence from this study that left-to-right TCD is linked to detrimental effects (Fig. 3a) for performance supports the importance of

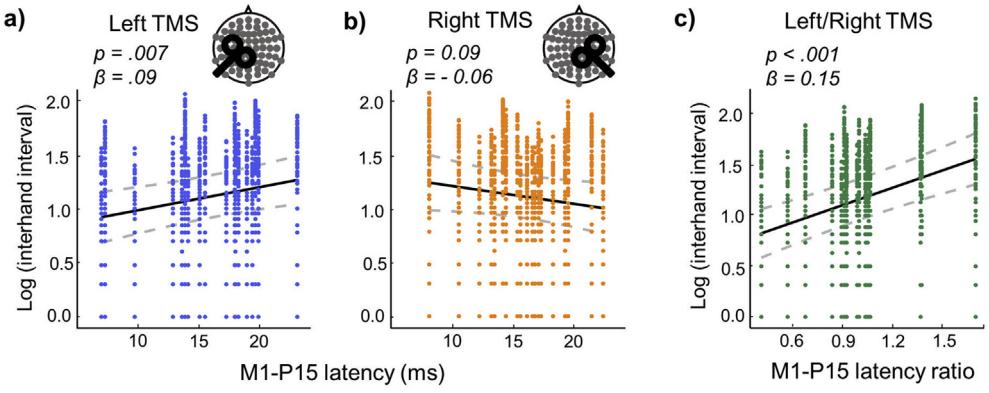

Fig. 4. Asymmetric transcallosal conduction delay predicts finer bimanual coordination. The relationship between M1-P15 latency and performance in the in-phase bimanual coordination task depends on the stimulated hemisphere. a) When TMS is delivered over M1 in the dominant hemisphere (left TMS), shorter M1-P15 latency is associated with finer bimanual coordination (positive relationship between M1-P15 latency and interhand interval). b) Conversely, when TMS is applied over M1 in the nondominant hemisphere (right TMS), shorter M1-P15 latency is associated with worse bimanual coordination (negative relationship between M1-P15 latency and interhand interval). c) The interhand interval is best predicted by the ratio of M1-P15 latency following left TMS to M1-P15 latency following right TMS, indicating that a shorter conduction delay from the dominant M1 to the nondominant M1 than in the opposite direction is associated with finer bimanual coordination. Fitted curves (linear trends) were drawn by applying a smoothed spline to predicted values—obtained by a bootstrap procedure with n = 500 simulations—in the LMMs. Dashed lines represent the 95% confidence interval.

interhemispheric timing in signal transmission. However, the evidence that asymmetric TCD is beneficial for performance is not fully consistent with the interhemispheric independence hypothesis.

Interestingly, the stimulation of the dPMC produced an index of TCD, i.e., dPMC-P15, which was different from M1-P15 (Fig. S1), was not linked to peripherally measured interhemispheric inhibition (Fig. S3) and was not linked to bimanual performance (Table S5). This finding is not surprising, given previous studies showing the involvement of dPMC in antiphase rather than in-phase bimanual movements, as the ones performed here [25,26]. The stimulation of the dPMC was achieved by moving the target forward by 15 mm from the M1 coordinates. Although this is a short distance that may include a region of overlap between M1 and dPMC, it corresponds to the distance of the foci of activation in M1 and in dPMC during motor tasks [31], and it is sufficient to target separate cortical areas with TMS [59]. These data suggest that the relation between TCD and bimanual performance may be highly specific for M1, possibly due to the type of task employed in this study.

Our results raise the intriguing question of how asymmetric TCD can be beneficial for performance. A possibility relates to mechanisms of competition between hemispheres. Such mechanisms have been previously proposed for both motor and cognitive systems [60,61]. According to the interhemispheric competition hypothesis [61], the function of the CC is to send inhibitory signals from each hemisphere to the other to avoid incoming interfering signals from homologous areas [61]. Although temporal aspects of communications are not addressed in the proposed framework, it is possible that an advantage in the timing of inhibition, i.e., one hemisphere is faster at sending signals to the other hemisphere, which may contribute to the definition of the "winner" of the competition, i.e., the dominant hemisphere. In this case, a longer TCD for the interfering signal (i.e., from the nondominant hemisphere) would facilitate the leading of the dominant hemisphere. Interestingly, an asymmetric timing of information transfer may facilitate competition not only when signals induce functional inhibition but also when they induce functional facilitation.

The execution of bilateral movements activates both sides of the motor system and requires an efficient interaction to reach high temporal synchronization. According to the model of neural cross-talk, motor commands are sent from each side both to the contralateral side of the corticospinal tract and, in a mirror version, to the ipsilateral side [62–64]. Pathways allowing this interaction include interhemispheric connections through the CC and subcortical pathways [65]. The relative conduction delay in each direction of the CC tract may affect how the signals from the two hemispheres interact and potentially interfere with each other. In this case, better bimanual coordination with more efficient signal transmission from the left M1 is in line with the well-known dominant role of the left hemisphere in the performance of bimanual movements and in movement sequences [66–68].

Considering that M1-P15 reflects a functional inhibitory signal, one possible mechanism is that prompt suppression of the nondominant motor area, conveyed through the CC as a functional inhibitory signal, may increase the efficiency of cross-talk at the corticospinal level, thus improving temporal coordination. In this case, information transfer through the CC would not be necessary to perform bimanual movements, but it would optimize their coordination. Accordingly, previous studies have shown that the CC contributes to temporal control of in-phase discrete movements, although CC integrity is not essential for this task, as it can be performed after callosotomy and by acallosal patients [69,70].

Alternatively, information transfer through the CC during the bimanual task may have a facilitatory function, rather than the inhibitory function that we observed during the iSP paradigm. Therefore, cross-talk would occur at the cortical level. This possibility cannot be ruled out because we did not record TEPs during the bimanual task. Nevertheless, faster signal transmission from the dominant hemisphere than from the nondominant hemisphere would still pose an advantage in the case of transcallosal functional facilitation, reducing the interference effects of intruding commands. Altogether, finer bimanual coordination would be reached when the transmission was asymmetric and gave a temporal advantage to the signal from the dominant hemisphere over the nondominant hemisphere, regardless of the information conveyed (i.e., either functional inhibition or signal transmission).

Furthermore, hemispheric asymmetry in M1-P15 latency may arise from asymmetry in the structure of callosal connections, thus expanding the notion of transcallosal cross-talk from a functional to a structural meaning. It can be suggested that asymmetric connectivity, in which only one direction of information processing is optimized, may be a consequence of the spatial and metabolic constraints that have limited evolutionary growth of the CC relative to brain size [71–73]. We speculate that this optimization would improve directional information transfer from the dominant to the nondominant hemisphere, creating the basis for hemispheric dominance.

The development of a noninvasive measure of TCD opens several new opportunities to study cortical connectivity and hemispheric asymmetries. First, it allows to run a thorough investigation of the inter-hemispheric mechanisms for other types of bimanual movements. Importantly, this approach can be extended to other cognitive domains involving other regions of the CC and other major intrahemispheric tracts. Eventually, it will be possible to integrate new knowledge on TCD in theoretical and computational models of interhemispheric interactions.

Data availability

The data that support the findings of this study are available from the authors on reasonable request.

CRediT authorship contribution statement

Marta Bortoletto: Conceptualization, Investigation, Formal analysis, Writing - original draft, Supervision. **Laura Bonzano:** Conceptualization, Formal analysis, Writing - original draft. **Agnese Zazio:** Investigation, Formal analysis, Visualization, Writing - original draft. **Clarissa Ferrari:** Formal analysis, Writing - review & editing. **Ludovico Pedullà:** Formal analysis. **Roberto Gasparotti:** Investigation, Resources. **Carlo Miniussi:** Conceptualization, Resources, Writing - review & editing. **Marco Bove:** Conceptualization, Writing - original draft.

Declaration of competing interest

The authors declare no competing interests.

Acknowledgments

This work was supported by Italian Multiple Sclerosis Foundation (FISM) Grant 2016/R/2 and Grant 2019/R-Multi/009. We would like to thank Alice Bollini and Simona Finazzi for their support with data acquisition.

Appendix A. Supplementary data

Supplementary data to this article can be found online at https://doi.org/10.1016/j.brs.2021.02.002.

References

[1] Ringo JL, Doty RW, Demeter S, Simard PY. Time is of the essence: a conjecture that hemispheric specialization arises from interhemispheric conduction delay. Cerebr Cortex 1994;4:331–43.

[2] Phillips KA, Stimpson CD, Smaers JB, Raghanti MA, Jacobs B, Popratiloff A, et al. The corpus callosum in primates: processing speed of axons and the evolution of hemispheric asymmetry. Proc Roy Soc B Biol Sci 2015;282. https://doi.org/10.1098/rspb.2015.1535.

[3] Karolis VR, Corbetta M, Thiebaut de Schotten M. The architecture of functional lateralisation and its relationship to callosal connectivity in the human brain. Nat Commun 2019;10:1–9. https://doi.org/10.1038/s41467-019-09344-1.

[4] Ferbert A, Priorit A, Rothwell JC, Day BL, Colebatchi JG, Marsden CD. Interhemispheric inhibition of the human motor cortex. J Physiol 1992;453:525–46.

[5] Hoptman MJ, Davidson RJ. How and why do the two cerebral hemispheres interact? Psychol Bull 1994;116:195–219. https://doi.org/10.1037/0033-2909.116.2.195.

[6] Cherbuin N, Brinkman C. Efficiency of callosal transfer and hemispheric interaction. Neuropsychology 2006;20:178–84. https://doi.org/10.1037/0894-4105.20.2.178.

[7] Marzi CA, Bisiacchi P, Nicoletti R. Is interhemispheric transfer of visuomotor information asymmetric? Evidence from a meta-analysis. Neuropsychologia 1991;29:1163–77. https://doi.org/10.1016/0028-3932(91)90031-3.

[8] Chaumillon R, Blouin J, Guillaume A. Eye dominance influences triggering action: the Poffenberger paradigm revisited. Cortex 2014;58:86–98. https://doi.org/10.1016/j.cortex.2014.05.009.

[9] Chaumillon R, Blouin J, Guillaume A. Interhemispheric transfer time asymmetry of visual information depends on eye dominance: an electrophysiological study. Front Neurosci 2018;12:1–19. https://doi.org/10.3389/fnins.2018.00072.

[10] Davidson T, Tremblay F. Hemispheric differences in corticospinal excitability and in transcallosal inhibition in relation to degree of handedness. PLoS One 2013;8:1–9. https://doi.org/10.1371/journal.pone.0070286.

[11] Trompetto C, Bove M, Marinelli L, Avanzino L, Buccolieri A, Abbruzzese G. Suppression of the transcallosal motor output: a transcranial magnetic stimulation study in healthy subjects. Exp Brain Res 2004;158:133–40. https://doi.org/10.1007/s00221-004-1881-6.

[12] Fling BW, Benson BL, Seidler RD. Transcallosal sensorimotor fiber tract structure-function relationships. Hum Brain Mapp 2013;34:384–95. https://doi.org/10.1002/hbm.21437.

[13] Meyer BU, Röricht S, Woiciechowsky C. Topography of fibers in the human corpus callosum mediating interhemispheric inhibition between the motor cortices. Ann Neurol 1998;43:360–9. https://doi.org/10.1002/ana.410430314.

[14] Meyer BU, Röricht S, Von Einsiedel HG, Kruggel F, Weindl A. Inhibitory and excitatory interhemispheric transfers between motor cortical areas in normal humans and patients with abnormalities of the corpus callosum. Brain 1995;118:429–40. https://doi.org/10.1093/brain/118.2.429.

[15] Ni Z, Leodori G, Vial F, Zhang Y, Avram AV, Pajevic S, et al. Measuring latency distribution of transcallosal fibers using transcranial magnetic stimulation. Brain Stimul 2020;13:1453–60. https://doi.org/10.1016/j.brs.2020.08.004.

[16] Bortoletto M, Veniero D, Thut G, Miniussi C. The contribution of TMS – EEG coregistration in the exploration of the human cortical connectome. Neurosci Biobehav Rev 2015;49:114–24. https://doi.org/10.1016/j.neubiorev.2014.12.014.

[17] Ilmoniemi RJ, Virtanen CAJ, Ruohonen J, Karhu J, Aronen HJ, Näätänen R, et al. 1997_Ilmoniemi_Neuronal responses to magnetic stimulation. Neuroreport 1997;8:3537–40.

[18] Komssi S, Aronen HJ, Huttunen J, Kesäniemi M, Soinne L, Nikouline VV, et al. Ipsi- and contralateral EEG reactions to transcranial magnetic stimulation. Clin Neurophysiol 2002;113:175–84.

[19] Cracco RQ, Amassian VE, Maccabee PJ, Cracco JB. Comparison of human transcallosal responses evoked by magnetic coil and electrical stimulation. Electroencephalogr Clin Neurophysiol Evoked Potentials 1989;74:417–24. https://doi.org/10.1016/0168-5597(89)90030-0.

[20] Zarei M, Johansen-Berg H, Smith S, Ciccarelli O, Thompson AJ, Matthews PM. Functional anatomy of interhemispheric cortical connections in the human brain. J Anat 2006;209:311–20. https://doi.org/10.1111/j.1469-7580.2006.00615.x.

[21] Bonzano L, Tacchino A, Roccatagliata L, Abbruzzese G, Mancardi GL, Bove M. Callosal contributions to simultaneous bimanual finger movements. J Neurosci 2008;28:3227–33. https://doi.org/10.1523/JNEUROSCI.4076-07.2008.

[22] Ouimet C, Jolicœur P, Lassonde M, Ptito A, Paggi A, Foschi N, et al. Bimanual crossed-uncrossed difference and asynchrony of normal, anterior- and totally-split-brain individuals. Neuropsychologia 2010;48:3802–14. https://doi.org/10.1016/j.neuropsychologia.2010.09.003.

[23] Eliassen JC, Baynes K, Gazzaniga MS. Anterior and posterior callosal contributions to simultaneous bimanual movements of the hands and fingers. Brain 2000;123:2501–11. https://doi.org/10.1093/brain/123.12.2501.

[24] Chen J-TT, Lin Y-YY, Shan D-EE, Wu Z-AA, Hallett M, Liao K-KK. Effect of transcranial magnetic stimulation on bimanual movements. J Neurophysiol 2005;93:53–63. https://doi.org/10.1152/jn.01063.2003.

[25] Liuzzi G, Hörniß V, Zimerman M, Gerloff C, Hummel FC. Coordination of uncoupled bimanual movements by strictly timed interhemispheric connectivity. J Neurosci 2011;31:9111–7. https://doi.org/10.1523/JNEUROSCI.0046-11.2011.

[26] Meyer-Lindenberg A, Ziemann U, Hajak G, Cohen L, Berman KF. Transitions between dynamical states of differing stability in the human brain. Proc Natl Acad Sci U S A 2002;99:10948–53. https://doi.org/10.1073/pnas.162114799.

[27] Oldfield RC. The assessment and analysis of handedness: the Edinburgh inventory. Neuropsychologia 1971;9:97–113. https://doi.org/10.1016/0028-3932(71)90067-4.

[28] Signori A, Sormani MP, Schiavetti I, Bisio A, Bove M, Bonzano L. Quantitative assessment of finger motor performance: normative data. PLoS One 2017;12:1–13. https://doi.org/10.1371/journal.pone.0186524.

[29] Bove M, Tacchino A, Novellino A, Trompetto C, Abbruzzese G, Ghilardi MF. The effects of rate and sequence complexity on repetitive finger movements. Brain Res 2007;1153:84–91. https://doi.org/10.1016/j.brainres.2007.03.063.

[30] Bonzano L, Sormani MP, Tacchino A, Abate L, Lapucci C, Mancardi GL, et al. Quantitative assessment of finger motor impairment in multiple sclerosis. PLoS One 2013;8:e65225. https://doi.org/10.1371/journal.pone.0065225.

[31] Mayka MA, Corcos DM, Leurgans SE, Vaillancourt DE. Three-dimensional locations and boundaries of motor and premotor cortices as defined by functional brain imaging: a meta-analysis. Neuroimage 2006;31:1453–74. https://doi.org/10.1016/j.neuroimage.2006.02.004.

[32] Giovannelli F, Borgheresi A, Balestrieri F, Zaccara G, Viggiano MP, Cincotta M, et al. Modulation of interhemispheric inhibition by volitional motor activity: an ipsilateral silent period study. J Physiol 2009;587:5393–410. https://doi.org/10.1113/jphysiol.2009.175885.

[33] Rossini PM, Barker AT, Berardelli A, Caramia MD, Caruso G, Cracco RQ, et al. Non-invasive electrical and magnetic stimulation of the brain, spinal cord, roots and peripheral nerves: basic principles and procedures for routine clinical and research application: an updated report from an I.F.C.N. Committee. Clin Neurophysiol 1994;91:79–92.

[34] Veniero D, Bortoletto M, Miniussi C. Clinical Neurophysiology TMS-EEG co-registration : on TMS-induced artifact. Clin Neurophysiol 2009;120:1392–9. https://doi.org/10.1016/j.clinph.2009.04.023.

[35] Smith SM, Jenkinson M, Woolrich MW, Beckmann CF, Behrens TEJ, Johansen-Berg H, et al. Advances in functional and structural MR image analysis and implementation as FSL. Neuroimage 2004;23:208–19. https://doi.org/10.1016/j.neuroimage.2004.07.051.

[36] Basser PJ. Inferring microstructural features and the physiological state of tissues from diffusion weighted images. NMR Biomed 1995;8:333–44.

[37] Bonzano L, Tacchino A, Brichetto G, Roccatagliata L, Dessypris A, Feraco P, et al. Upper limb motor rehabilitation impacts white matter microstructure in multiple sclerosis. Neuroimage 2014;90:107–16. https://doi.org/10.1016/j.neuroimage.2013.12.025.

[38] Beaulieu C. The biological basis of diffusion anisotropy. Elsevier Inc.; 2009. https://doi.org/10.1016/B978-0-12-374709-9.00006-7.

[39] Smith SM, Jenkinson M, Johansen-Berg H, Rueckert D, Nichols TE, Mackay CE, et al. Tract-based spatial statistics: voxelwise analysis of multi-subject diffusion data. Neuroimage 2006;31:1487–505. https://doi.org/10.1016/j.neuroimage.2006.02.024.

[40] Mori S, Wakana S, Van Zijl PCM, Nagae-Poetscher LM. MRI atlas of human white matter. Elsevier; 2005.

[41] Delorme A, Makeig S. EEGLAB: an open source toolbox for analysis of single-trial EEG dynamics including independent component analysis. J Neurosci Methods 2004;134:9–21. https://doi.org/10.1016/j.jneumeth.2003.10.009.

[42] Oostenveld R, Fries P, Maris E, Schoffelen JM. FieldTrip: open source software for advanced analysis of MEG, EEG, and invasive electrophysiological data. Comput Intell Neurosci 2011;2011. https://doi.org/10.1155/2011/156869.

[43] Mutanen TP, Metsomaa J, Liljander S, Ilmoniemi RJ. Automatic and robust noise suppression in EEG and MEG: the SOUND algorithm. Neuroimage 2018;166:135–51. https://doi.org/10.1016/j.neuroimage.2017.10.021.

[44] Mutanen TP, Kukkonen M, Nieminen JO, Stenroos M, Sarvas J, Ilmoniemi RJ. Recovering TMS-evoked EEG responses masked by muscle artifacts. Neuroimage 2016;139:157–66. https://doi.org/10.1016/j.neuroimage.2016.05.028.

[45] Biabani M, Fornito A, Mutanen TP, Morrow J, Rogasch NC. Characterizing and minimizing the contribution of sensory inputs to TMS-evoked potentials. Brain Stimul 2019;12:1537–52. https://doi.org/10.1016/j.brs.2019.07.009.

[46] Kuo YL, Dubuc T, Boufadel DF, Fisher BE. Measuring ipsilateral silent period: effects of muscle contraction levels and quantification methods. Brain Res 2017;1674:77–83. https://doi.org/10.1016/j.brainres.2017.08.015.

[47] Galecki A, Burzykowski T. Linear mixed-effects models using R: a Step-by-Step approach. Springer-Verlag New York; 2013. https://doi.org/10.1007/978-1-4614-3900-4.

[48] R Core Team. R. A language and environment for statistical computing. Austria: R Found Stat Comput Vienna; 2013. https://www.r-project.org.

[49] Caminiti R, Carducci F, Piervincenzi C, Battaglia-Mayer A, Confalone G, Visco-Comandini F, et al. Diameter, length, speed, and conduction delay of callosal axons in macaque monkeys and humans: comparing data from histology and magnetic resonance imaging diffusion tractography. J Neurosci 2013;33:14501–11. https://doi.org/10.1523/JNEUROSCI.0761-13.2013.

[50] Burnham KP, Anderson DR. Model selection and multimodel inference: a practical information-theoretic approach. second ed., vol. 172; 2002. https://doi.org/10.1016/j.ecolmodel.2003.11.004.

[51] Burnham KP, Anderson DR. Multimodel inference: understanding AIC and BIC in model selection. Sociol Methods Res 2004;33:261–304. https://doi.org/10.1177/0049124104268644.
[52] Avanzino L, Bove M, Trompetto C, Tacchino A, Ogliastro C, Abbruzzese G. 1-Hz repetitive TMS over ipsilateral motor cortex influences the performance of sequential finger movements of different complexity. https://doi.org/10.1111/j.1460-9568.2008.06086.x; 2008. 27, 1285-1291.
[53] Mueller JK, Grigsby EM, Prevosto Iii FWP V, Rao H, Deng Z De, et al. Simultaneous transcranial magnetic stimulation and single-neuron recording in alert non-human primates. Nat Neurosci 2014;17:1130–6. https://doi.org/10.1038/nn.3751.
[54] Fujiyama H, Soom J Van, Rens G, Gooijers J, Leunissen XI, Levin O, et al. Age-related changes in frontal network structural and functional connectivity in relation to bimanual movement control. J Neurosci 2016;36:1808–22. https://doi.org/10.1523/JNEUROSCI.3355-15.2016.
[55] Koganemaru S, Mima T, Nakatsuka M, Ueki Y, Fukuyama H, Domen K. Human motor associative plasticity induced by paired bihemispheric stimulation. J Physiol 2009;587:4629–44. https://doi.org/10.1113/jphysiol.2009.174342.
[56] Swinnen SP, Jardin K, Muelenbroek R. Between-limb asynchronies during bimanual coordination : effects of manual dominance and attentional cueing. Neuropsychologia 1996;34:1203–13.
[57] Swinnen SP, Jardin K, Meulenbroek R, Dounskaia N, Van Den Brandt MH. Egocentric and allocentric constraints in the expression of patterns of inter-limb coordination. J Cognit Neurosci 1997;9:348–77. https://doi.org/10.1162/jocn.1997.9.3.348.
[58] Swinnen SP, Jardin K, Verschueren S, Meulenbroek R, Franz L, Dounskaia N, et al. Exploring interlimb constraints during bimanual graphic performance: effects of muscle grouping and direction. Behav Brain Res 1998;90:79–87.
[59] Romero MC, Davare M, Armendariz M, Janssen P. Neural effects of transcranial magnetic stimulation at the single-cell level. Nat Commun 2019;10:1–11. https://doi.org/10.1038/s41467-019-10638-7.
[60] Kinsbourne M. Hemi-neglect and hemisphere rivalry. Adv Neurol 1977;18:41–9.
[61] Kinsbourne M. Mechanisms of hemispheric interaction in man. Hemispheric Disconnection Cereb Funct 1974;XIII:260–85.
[62] Cattaert D, Semjen A, Summers JJ. Simulating a neural cross-talk model for between-hand interference during bimanual circle drawing. Biol Cybern 1999;81:343–58. https://doi.org/10.1007/s004220050567.
[63] Aramaki Y, Honda M, Sadato N. Suppression of the non-dominant motor cortex during bimanual symmetric finger movement: a functional magnetic resonance imaging study. Neuroscience 2006;141:2147–53. https://doi.org/10.1016/j.neuroscience.2006.05.030.
[64] Ziemann U, Hallett M. Hemispheric asymmetry of ipsilateral motor cortex activation during unimanual motor tasks: further evidence for motor dominance. Clin Neurophysiol 2001;112:107–13. https://doi.org/10.1016/S1388-2457(00)00502-2.
[65] Ivry RB, Hazeltine E. Subcortical locus of temporal coupling in the bimanual movements of a callosotomy patient. Hum Mov Sci 1999;18:345–75. https://doi.org/10.1016/S0167-9457(99)00014-7.
[66] Geffen GM, Jones DL, Geffen LB. Interhemispheric control of manual motor activity. Behav Brain Res 1994;64:131–40. https://doi.org/10.1016/0166-4328(94)90125-2.
[67] Serrien DJ, Ivry RB, Swinnen SP. Dynamics of hemispheric specialization and integration in the context of motor control. Nat Rev Neurosci 2006;7:160–7. https://doi.org/10.1038/nrn1849.
[68] Rueda-Delgado LM, Solesio-Jofre E, Serrien DJ, Mantini D, Daffertshofer A, Swinnen SP. Understanding bimanual coordination across small time scales from an electrophysiological perspective. Neurosci Biobehav Rev 2014;47:614–35. https://doi.org/10.1016/j.neubiorev.2014.10.003.
[69] Kennerley SW, Diedrichsen J, Hazeltine E, Semjen A, Ivry RB. Callosotomy patients exhibit temporal uncoupling during continuous bimanual movements. Nat Neurosci 2002;5:376–81. https://doi.org/10.1038/nn822.
[70] Gooijers J, Swinnen SP. Interactions between brain structure and behavior: the corpus callosum and bimanual coordination. Neurosci Biobehav Rev 2014;43:1–19. https://doi.org/10.1016/j.neubiorev.2014.03.008.
[71] Caminiti R, Ghaziri H, Galuske R, Hof PR, Innocenti GM. Evolution amplified processing with temporally dispersed slow neuronal connectivity in primates. Proc Natl Acad Sci U S A 2009;106:19551. https://doi.org/10.1073/pnas.0907655106. –6.
[72] Herculano-Houzel S, Mota B, Wong P, Kaas JH. Connectivity-driven white matter scaling and folding in primate cerebral cortex. Proc Natl Acad Sci U S A 2010;107:19008. https://doi.org/10.1073/pnas.1012590107. –13.
[73] Hopkins WD, Misiura M, Pope SM, Latash EM. Behavioral and brain asymmetries in primates: a preliminary evaluation of two evolutionary hypotheses. Ann N Y Acad Sci 2015;1359:65–83. https://doi.org/10.1111/nyas.12936.